



e-ISSN: 2319-8753 | p-ISSN: 2347-6710

# IJIRSET

International Journal of Innovative Research in  
**SCIENCE | ENGINEERING | TECHNOLOGY**

# INTERNATIONAL JOURNAL OF INNOVATIVE RESEARCH

IN SCIENCE | ENGINEERING | TECHNOLOGY

Volume 10, Special Issue 2, December 2021

**ISSN** INTERNATIONAL  
STANDARD  
SERIAL  
NUMBER  
INDIA

**Impact Factor: 7.569**

9940 572 462

6381 907 438

[ijirset@gmail.com](mailto:ijirset@gmail.com)

[www.ijirset.com](http://www.ijirset.com)

# Integration of 2-Dimensional-Convolutional Neural Network and Markov Random Field for Hyperspectral Image Classification

M. Preethi<sup>1</sup>, Dr.C.Velayutham<sup>2</sup>, Dr.S. Arumugaperumal<sup>3</sup>

(Research Scholar), Department of Computer Science, S.T. Hindu College, Nagercoil, Affiliated to Manonmaniam Sundaranar University, Tirunelveli, Tamil Nadu, India<sup>1</sup>

(Research supervisor), Head and Associate Professor Department of Computer Science, Aditanar College of arts and science, Tiruchendur, Affiliated to Manonmaniam Sundaranar University, Tirunelveli, Tamil Nadu, India<sup>2</sup>

(Research Joint Supervisors), Head and Associate Professor, Department of Computer Science, S.T. Hindu College, Nagercoil. Affiliated to Manonmaniam Sundaranar University, Tirunelveli, Tamil Nadu, India<sup>3</sup>

**ABSTRACT:** Hyperspectral imaging technology captures and analyzes image in continuous narrow spectral bands to produce a high dimensional Hyperspectral Image (HSI). Recently Many researchers used a Convolutional Neural Network (CNN) for classification but this proposed work is based on integrating 2-Dimensional-CNN (2D-CNN) and Markov Random Field (MRF) to improve the over-smoothing of classification results. The proposed techniques consist of two steps: In the first step, 2-D patches are extracted from an HSI. The extracted patches are given as input in 2D-CNN framework which is constructed for extracting the local spatial information and then extracted features are provided through fully connected layer. Finally, softmax activation function is used to train the classifier. In the second step, additionally the probabilistic classification map obtained in the first step can also be improved by placing a smoother prior on the labels, which is achieved by MRF. Experimental results on different hyperspectral images prove that proposed method is robust and offers more classification results than state-of-the-art method.

**KEYWORDS:** 2D-CNN, Hyperspectral image, Deep Learning, Spatial- Spectral.

## I. INTRODUCTION

Hyperspectral remote sensors capture image in hundreds of spectral bands, which span from the visible to infrared spectrum. It provides useful information for different materials. HSI is totally different from normal RGB image. Because HSI contains more spectral information about image but normal RGB image has three spectral bands. Each pixel in HSI is a high dimensional vector which is used to distinguish different landscapes. Due to the high dimensionality, classifying the pixel is not easy. HSI classification can be used in many applications, Such as Agriculture, Military, Surveillance and Environment monitoring [20], [33]. Many supervised methods have been applied in the machine learning for HSI classification in the last few decades. In general, these methods can be roughly divided into two categories: spectral based method [9], [10] and spectral-spatial based method. In spectral based method, Traditional spectral classification algorithms typically include K-nearest neighbors (KNN), Maximum likelihood, Support Vector Machine (SVM) [22], Multinomial Logistic Regression (MLR) [13] and Active Learning [14]. Later many spatial-spectral classification models were proposed to improve the classification performance. There are three main categories: The first category analyse the methods based on spatial feature extraction. In this approach, spatial features like texture [8] and structure [10] are extracted and then the spatial and spectral information can be combined, e.g., by utilizing composite kernels [4]. The second category consist patch based feature extraction method, which group neighboring pixels using data cube and then extracts features using a subspace learning techniques such as low-rank matrix factorization, dictionary learning or subspace clustering. The third category discusses the spatial information based on MRF model [32]. Recently, advanced multilayer neural network have been used for machine learning problems including classification or segmentation task [4], [5], [29], [30]. Among deep approaches, many researchers have been attracted CNN which extract spatial features, and integrated with spectral features for HSI

classification [6]. In addition, 3D-CNN was utilized to extract deep spectral-spatial feature directly from raw HSI [11]. Similarly [17], spectral-spatial classification for 3D-CNN used as inputs cubes of HSI with a small spatial size. These models discussed the thematic maps that can directly process raw HSI, whereas the classification accuracy of the CNN model decreases when the network becomes deeper.

## II. RELATED WORK

Lee et al. [14], have proposed a novel contextual deep CNN which can jointly extract the spectral and spatial information of hyperspectral images. The extracted feature map provided the rich spectral and spatial properties of the hyperspectral images and then given to fully connected layers that is used to eventually predict the corresponding label of each pixel vector. Kaiqiang Zhu et al [12], introduced a deep capsule network for hyperspectral image (HSI) classification to improve the performance of the conventional convolutional neural networks (CNNs). Wenchao Qi et al [31], have proposed a spectral-spatial cascaded 3D convolutional neural network (CNN) with a convolutional long short-term memory (CLSTM) network, called SSCC for HSI classification. This existing framework works cascaded 3D CNN which is used to learn the spectral-spatial features of HSIs and uses the CLSTM network to extract sequence features. Li Wang et al [17], proposed a spatial-spectral squeeze-and-excitation (SSSE) module. This existing modules is used to adaptively learn the weights for different spectral bands and for different neighboring pixels. Pedram Ghamisi et al. [24], proposed Self Improving CNN (SICNN), which is based on considering Fractional Order Darwinian Particle Swarm Optimization (FODPSO). The proposed approach addresses the main shortcoming of a CNN-based classification approach for hyperspectral data. Yue et al. [35], developed a 2-D and 3-D combined CNN. 2D-CNN is utilized for the feature extraction in the single band and 3D- CNN can simultaneously extract features for HSI. Lin Zhu et al. [19], proposed a Generative Adversarial Network (GAN), which contains a generative network and a discriminative network for HSI classification. Fahim Irfan Alam et al. [7], integrated the framework consisting of CNN and CRF which is used to classify hyper-spectral image by consider both spectral-spatial information. Akrem Sellami et al [1], proposed fused 3-D spectral-spatial deep neural networks for hyperspectral image classification. The proposed method introduced an unsupervised band selection method to avoid the problem of redundancy between spectral bands. Radhesyam Vaddi et al [26], combined data normalization and CNN for remote sensing hyperspectral image classification. Probabilistic Principal Component Analysis (PPCA) and Gabor filtering are used to extract the spatial-spectral information respectively. Finally classification accuracy obtained using simply designed CNN framework. Alkha Mohan et al [2], proposed a hybrid CNN classification technique. It extracts the spectral and spatial features for different window sizes using 3D-CNN. These 3D-CNN features are fused and given into a 2D-CNN. The combined features are used to improve the classification accuracy. In Muhammad Ahmada et al [23], a spatial prior generalized fuzziness extreme learning machine autoencoder (GFELM-AE) based active learning is proposed. The proposed method is extracted the spatial-spectral feature simultaneously. The classification accuracy is obtained by the proposed approach which is containing the more computational time. Qin Xu et al [25], designed multiscale convolution to extract the contextual feature for HSIs and then to employ the octave 3D-CNN which is used to reduce the spatial redundancy and enlarge the respective field.

### A. Contributions of our proposed approach

The key contribution of this work, inspired as follow by [18], a novel deep learned based 2D-CNN approach is utilized that uses convolutional layers to extract spectral and spatial information from hyperspectral data. The flow chart of the proposed approach is depicted in Fig. 1. In the first step of the proposed approach, we extract the 2-D patches as  $S \times S \times D$  from HSI where  $S \times S$  denotes spatial information and  $D$  denotes the Spectral information. They are given into 2D-CNN framework. There are three convolutional layers in the 2D-CNN. At the initial stage of 2D-CNN, 2-dimensional convolution filters with different size are simultaneously extracted the spatial feature maps. In 2D-CNN, max pooling layer and a fully connected (FC) layer is used. The combined feature maps are used as input to fully connected layer that predict the labels of the corresponding hyperspectral pixel vectors. Finally, the classification map is obtained using a soft-max activation function. The classification map obtained in the 2D-CNN can also be improved by MRF for refining the classification results.

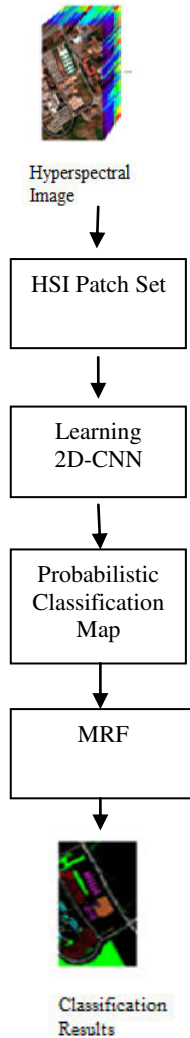


Fig. 1. Flowchart which shows the proposed 2D-CNN-MRF algorithm.

This paper is organized as follows: Proposed method is discussed in section II. In section III, experimental results on two benchmark HSIs are reported. Finally, conclusions are drawn in section IV.

### III. PROPOSED METHOD

In this work, the proposed approach of the 2D-CNN-MRF classification method are explained in detail and discuss on how to train the network and analyze what the 2D-CNN model extracts from HSI. Next, the spatial information is refined by MRF.

#### A. CNN operation

Recently, many researchers have been used deep learning based methods to the hyperspectral images and demonstrated the excellent performance [5]. With this model, a good representation of feature can be learned, which allows performing end to end classifications tasks.

The convolutional layer is introduced first. The value of a neuron  $v_{ij}^x$  at position  $x$  of the  $j^{th}$  feature map in the  $i^{th}$  layer is denoted as follows:



$$v_{ij}^x = g(b_{ij} + \sum_m \sum_{p=0}^{P_i-1} w_{ijm}^p v_{(i-1)m}^{x+p}) \quad (1)$$

where m indexes the feature map in the previous layer. ((i - 1)<sup>th</sup> layer) connected to the current feature map,  $w_{ijm}^p$  is the weight of position p connected to the m<sup>th</sup> feature map,  $P_i$  is the width of the kernel toward the spectral dimension, and  $b_{ij}$  is the bias of  $j^{th}$  feature map in  $i^{th}$  the layer.

B. 2D-CNN :

A complete 2-D CNN layer contains a convolutional layer and a pooling layer. The value of a neuron  $v_{ij}^{xy}$  at position (x,y) of the  $j^{th}$  feature map in the  $i^{th}$  layer is denoted as follows:

$$v_{ij}^{xy} = g(b_{ij} + \sum_m \sum_{p=0}^{P_i-1} \sum_{q=0}^{Q_i-1} w_{ijm}^{pq} v_{(i-1)m}^{(x+p)(y+q)}) \quad (2)$$

where m indexes the feature map in the previous layer ((i - 1)<sup>th</sup> layer) connected to the current feature map,  $w_{ijm}^{pq}$  is the is the weight of position (p, q) connected to the  $m^{th}$  feature map.  $P_i$  and  $Q_i$  are the height and the width of the spatial convolution kernel\_ and  $b_{ij}$  is the bias of  $j^{th}$  feature map in  $i^{th}$  the layer.

C. HSI Classification with 2D-CNN-MRF

We propose a novel method of 2D-CNN and MRF for HSI classification. First, we extract the 2D-patches from HSI data. The extracted patches are fed into 2D-CNN framework.

D. The proposed Architecture of the 2D-CNN

The Architecture of the 2D-CNN is displayed in figure 1. It contains seven layer including one input layer, three convolutional layer and three Rectified Linear Unit (ReLU) activation functions where fully connected layer is the output of the whole network. 2D-CNN can effectively analyze the spatial and spectral features among the neighboring patches of the input data. Fig.2. shows the detailed parameter setting for each layer.

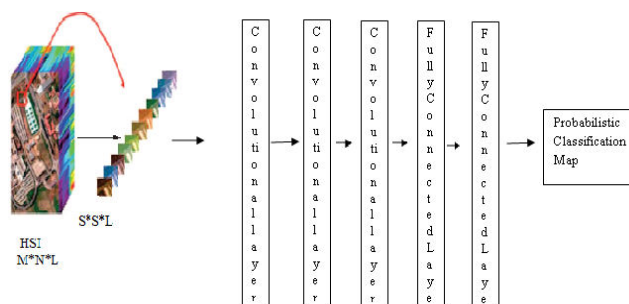


Fig. 2. The architecture of the 2D-CNN used as classifier.

E. 2D-CNN-MRF

In the final step, the probabilistic classification map of the 2D-CNN can also be improved using MRF framework. This framework is used for the interpixel class dependence assumption, which means that a pixel belonging to a class  $w_i$  is likely to have neighboring pixels belonging to the same class. The energy function encourages the labels of neighboring pixels to be close. Many algorithms has been proposed for encouraging the neighboring pixels such as the graph cut method [15], belief propagation [35] and message passing [30].

Specifically, probabilities label prediction  $\tilde{Y} \in R^{n \times K}$  (also called probabilistic map) on the whole dataset x obtained by 2D-CNN. Then, given the predicted values  $\tilde{y}$  replace  $P(y_i|x_i)$  with  $P(y_i|\tilde{y}_i)$ . Next, the final classification results are obtained by following optimization problem.

$$\hat{y} = \arg \max_{y \in K^n} \{ \sum_{i=1}^n (\log P(y_i|\tilde{Y}_i) + \log P(y)) \} \quad (3)$$

In our work, the log-likelihood  $\log P(y_i|\tilde{y}_i)$  is defined as

$$P(\tilde{Y}_i|y_i) = \sum_{k=1}^K 1\{y_i = k\} \log \tilde{y}_{ik} \quad (4)$$

Where  $1\{.\}$  is an indicator function.



$P(y)$  can be modeled with a MRF prior which means that the spatially adjacent pixels belong to the same class. This is formulated as

$$P(y) = \frac{1}{W} e^{\mu \sum_{i=1}^n \sum_{j \in N(i)} \delta(y_i - y_j)} \quad (5)$$

Where  $W$  is a normalization constant,  $\mu$  is the label smoothness parameter,  $N(i)$  is the neighboring pixels of pixel  $i$  and  $\delta(\cdot)$  is a function which is defined as:  $\delta(0) = 1$  and  $\delta(y) = -1$  for  $y \neq 0$ . It should be noted that the pairwise interaction terms  $\delta(y_i - y_j)$  obtain higher probability when neighboring labels are equal than when they are not equal. Our proposed method will further analyze the output obtained by the 3D-CNN. Then, the log-likelihood  $\log P((y_i | \tilde{y}_i)$  and on the label prior  $P(y)$ , the classification model can be given by

$$\hat{y} = \arg \max_{y \in K^n} \{ \sum_{i=1}^n \sum_{k=1}^K 1\{y_i = k\} \log \tilde{y}_{ik} + \mu \sum_{i=1}^n \sum_{j \in N(i)} \delta(y_i - y_j) \} \quad (6)$$

In this paper, we use the  $\alpha$ -expansion min-cut method [11] because of its good approximation performance and fast computational efficiency. To clarify the details of our classification algorithm, summarize the procedure in algorithm 1.

Input: HSI data  $H \in R^{h \times w \times d}$ , Training data  $D$ , label of patches  $y = \{y_1, y_2, \dots, y_n\}$ , Number of class labels  $K$ .

Output: Labels  $\hat{y}$ .

---



---

**Algorithm1. 2D-CNN-MRF Hyperspectral Image Classification**

---



---

1. for Each patches  $x_i \in R^{k \times k \times d}$  in  $H$  do
2.  $X = \{x_1, x_2, \dots, x_n\}$
3. While training samples  $i: 1 \rightarrow X$
4. Randomly select patch for  $D$  as training data and use the remaining as testing ones;
5.  $D_{l(k)}^{(k)} = \{(x_1, y_1), \dots, (x_{l(k)}, y_{l(k)})\}$ ;
6. Perform three convolution operation using Eq. (2);
7. Perform ReLU operation  $f(x) = \max(0, x)$ ;
8. Generate feature map using convolution and ReLU operation;
9. Compute soft-max activation  $a = \frac{\exp(o)}{\sum_k \exp(o_k)}$ ;
10. end while
11. end for
12. Compute probabilistic classification map  $y$  on the whole data set  $H$  using trained 2D-CNN;
13. Compute the classification label  $\hat{y}$  using Eq. 6.

#### IV. EXPERIMENTAL RESULTS AND DISCUSSION

In this section, the proposed approach of 2D-CNN-MRF is validated on two benchmark datasets, namely Indian pines data and Pavia University data. All the experiments were implemented in Matlab R2019a on a PC with 64 GB RAM. The proposed approach is validated by following the criteria [1]: Overall accuracy (OA), Average Accuracy (AA), and Statistically kappa coefficient ( $k$ ). Specifically, OA represents the number of correctly classified samples divided by the total number of test samples, AA denotes the average of individual class accuracies and kappa coefficient ( $K$ ) is a statistical measurement based on the confusion matrix of different classes.

##### A. Classification of Indian pines data

This data set was gathered by Airborne Visible/Infrared Imaging Spectrometer (AVIRIS) sensor over the Indian Pines test site in Northwestern Indiana in June 1992. The original dataset contains 220 spectral reflectance bands in the wavelength range 0.4–2.5  $\mu\text{m}$ , and the spatial dimension is 145×145. The ground truth contains 16 land cover classes in Table I.



15<sup>th</sup> & 16<sup>th</sup> September 2021

Organized by

Department of Computer Science, Parvathy's Arts and Science College, Dindigul, Tamilnadu, India

TABLE I  
SAMPLES OF THE INDIAN PINES DATA SET, INCLUDING THE NAME, THE NUMBER OF TOTAL SAMPLES FOR EACH CLASS.

Class		Samples
No	Name	Total
2	Alfalfa	46
	Corn-no till	1428
3	Corn -min till	830
4	Corn	237
5	Grass-pasture	483
6	Grass-tree	730
7	Grass-Pasture-mowed	28
8	Hay-Windrowed	478
9	Oat	20
10	Soybean-no till	972
11	Soybean-min till	2455
12	Soybean-clean	593
13	Wheat	205
14	Woods	1265
15	Buildings-Grass-Tree	386
16	Stone-Steel-Towers	93
Total		10249

To evaluate the validity of our proposed 2D-CNN-MRF method, randomly we choose 50% of the available labeled samples for training data, and then the remaining samples in each class are used to test. The proposed method have several parameters such as the sample patch size k, network depth, network width (the number of kernels in each convolutional layer), the kernel size in each convolutional layer, the kernel size in each max pooling layer and the number of nodes in the fully connected layers. In this experiment, several parameters are fixed as follows (also shown in figure 1).

1. The network depth is 5 (not including the input layer): three convolutional layers, ReLU layers and two fully connected layers.
2. The kernel size in the three convolutional layers is set as 2 and 1 respectively, and the number of kernels is set as 20 and 35 respectively.
3. There are 200 and 100 nodes for two fully connected layers respectively.

TABLE II  
OVERALL, AVERAGE ACCURACIES (%) AND KAPPA STATISTICS OF COMPARISON AND PROPOSED METHODS ON THE INDIAN PINES IMAGE

Class	SVM	SVM-3D	CNN	MLRsubMLL	CNN-MRF	2D-CNN-MRF
1	46.34	93.55	34.15	22.22	95.17	97.75
2	69.03	44.80	89.57	56.22	89.57	100.00
3	53.41	77.06	88.62	7.38	90.36	98.32
4	15.96	89.64	98.12	51.85	98.12	89.78
5	89.63	83.97	94.01	80.83	94.93	74.26
6	97.72	89.65	95.59	99.49	95.74	87.37
7	36.00	74.00	76.00	18.18	76.00	100.00
8	98.60	98.49	98.48	100	98.84	100.00
9	0	100	100	0	100	100.00
10	65.33	65.52	91.99	42.21	94.15	100.00
11	84.16	60.37	95.02	97.05	96.42	100.00
12	68.48	82.53	87.43	48.95	89.49	100.00
13	94.57	94.74	98.37	100	99.46	96.29
14	98.51	88.40	97.98	100	98.07	100.00
15	44.38	87.06	89.91	12.66	92.22	100.00
16	93.98	97.44	98.80	74.32	98.80	100.00
OA	59.12	72.51	93.50	70.88	94.62	97.65
AA	74.01	84.58	89.65	55.82	90.26	96.48
Kappa	54.62	69.11	92.28	65.50	93.40	96.67



For the above experimental settings, the proposed method was compared with current mainstream methods and calls these methods SVM, SVM-3D, MLRsubMLL, CNN, and CNN-MRF respectively. From Table II, analyze two main results such as CNN-MRF and 2D-CNN-MRF. In deep learning methods, CNN, CNN-MRF, and 2D-CNN-MRF achieve the best performance in terms of the three criteria (OA, AA, and K). First, SVM, SVM-3D, MLRsubMLL, CNN and CNN-MRF achieve poor classification results compared with 2D-CNN-MRF methods. Secondly, by using the MRF on the neighboring labels, the classification performance can be dramatically improved. The 2D-CNN-MRF method can be used to extract the spectral and spatial information in a HSI simultaneously. Finally from Fig 3, conclude that, for this dataset, our 2D-CNN-MRF approach achieves the best performance in terms of overall accuracy.

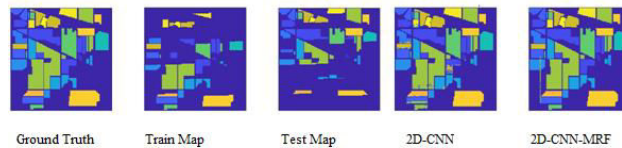


Fig. 3. Classification result of proposed Approach for Indian Pines dataset

The OA of each method is showed in Fig 4, from which observe that 2D-CNN-MRF method achieves the best performance in all cases. Meanwhile, CNN-MRF, and CNN obtain second and third highest OA, respectively.

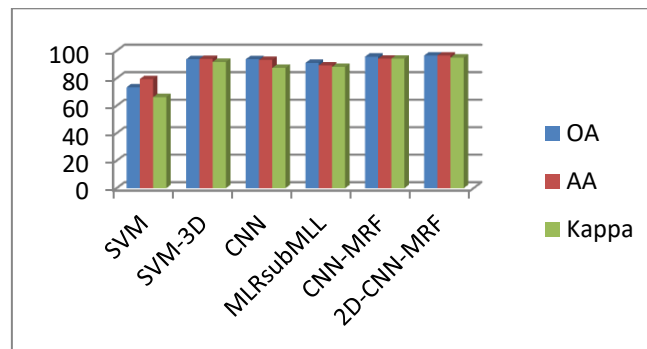


Fig. 4. OA, AA and Kappa achieved by comparison method and proposed approach for Indian Pines dataset

### B. Classification of Pavia University data

This dataset was acquired by the Reflective Optics System Imaging Spectrometer (ROSIS) over the urban area of the University of Pavia, northern Italy, on July 8, 2002. This dataset contain 103 spectral bands and the spatial dimension is 610x340. There are 9 land cover classes in this dataset and the number of each class is displayed in Table III.

TABLE III  
SAMPLES OF THE PAVIA UNIVERSITY DATA SET, INCLUDING THE NAME, THE NUMBER OF TOTAL SAMPLES FOR EACH CLASS.

Class		Samples
No	Name	Total
1	Asphalt	6631
2	Meadows	18,649
3	Gravel	2099
4	Trees	3064
5	Painted metal	1345
6	sheets	5029
7	Bare Soil	1330
8	Bitumen	3682
9	Self Blocking Bricks Shadows	947
Total		42,776



To evaluate the our proposed 2D-CNN-MRF method, randomly we choose 50% of the available labeled samples for training data, and then the remaining samples in each class are used to test.

TABLE IV  
OVERALL, AVERAGE ACCURACIES (%) AND KAPPA STATISTICS OF ALL COMPARISON AND PROPOSED METHODS ON THE PAVIA UNIVERSITY IMAGE TEST SET.

Class	SVM	SVM-3D	CNN	MLRsub-MLL	CNN-MRF	2D-CNN-MRF
1	74.78	94.09	96.78	87.07	97.92	97.41
2	69.75	94.92	84.82	96.97	97.38	98.18
3	71.54	88.87	86.69	77.27	87.66	100
4	92.79	96.45	94.18	83.90	98.97	91.66
5	96.86	99.61	97.47	99.54	99.92	92.18
6	67.27	95.56	96.31	99.40	92.00	100
7	75.43	95.63	91.40	94.50	85.27	100
8	67.68	81.64	91.93	64.83	91.54	100
9	98.13	99.89	99.34	99.78	97.13	96.56
OA	73.41	93.81	93.80	91.13	95.68	96.54
AA	79.36	94.07	93.28	89.25	94.20	96.44
Kappa	66.23	91.84	87.52	88.19	94.26	95.01

From Table IV and Figure 5, conclude that, for this dataset, our proposed approach achieves the best performances in terms of the three criteria. By using the 2D-CNN-MRF obtains good classification accuracy in terms of the OA compared with the CNN-MRF. The performance enhancement is achieved from using a 2D-CNN that jointly extracts spatial-spectral information of the hyperspectral data. The main reason is that the combined with 2D-CNN with MRF, which can encourage neighboring pixels to have the same class label. The result has been shown that MRF can help to greatly improve the classification accuracy in HSI task.

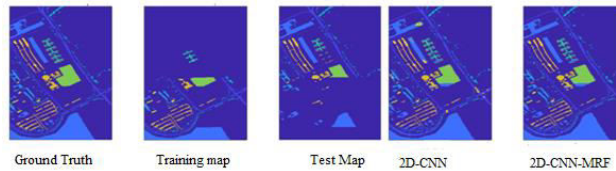


Fig. 5. Classification result of proposed Approach for Pavia University dataset

The OA of each method is showed in Figure 6, from which observe that 2D-CNN-MRF method achieves the best performance in all cases. Meanwhile, CNN-MRF and CNN obtain second and third highest OA, respectively.

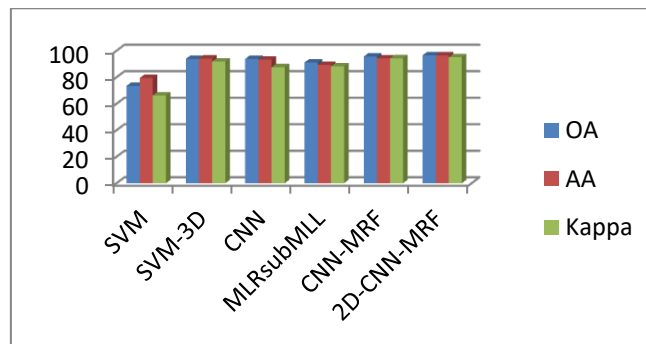


Fig. 6. OA, AA and Kappa achieved by comparison method and proposed approach for Pavia University dataset

## V. CONCLUSION

To improve the HSI classification, a 2D-CNN framework has been constructed that extract both spectral- spatial information contained within HSI data in this work. The extracted features are given to the fully connected layer. Then, softmax function is used to train the deep classifier. Finally, the resulting 2D feature map can also be improved by placing a smoother prior on the labels, which is achieved by MRF for refining the classification result. The proposed method of 2D-CNN-MRF provided the best classification accuracy of HSI data. The proposed method of 2D-CNN-MRF approach compared with three state-of-the-art deep learning based HSI classification methods, on two popular HSI benchmark data sheets. The experimental studies showed that the proposed method of 2D-CNN-MRF based HSI classification achieved the best overall accuracy on all the two datasets. In future work, we will concentrate how to reduce running time of the algorithm and application of the proposed method across variety of HSI datasets.

## REFERENCES

- [1] Akrem Sellami, Ali Ben Abbes, Vincent Barra d, and Imed Riadh Farah, "Fused 3-D spectral-spatial deep neural networks and spectral clustering for hyperspectral image classification," *Pattern Recognition Letters*, vol. 138, pp. 594–600, 2020.
- [2] Alkha Mohan, and Venkatesan M, "HybridCNN based hyperspectral image classification using multiscale spatiospectral features," *Infrared Physics and Technology*, vol. 108, Elsevier 2020.
- [3] Cao, X., Xu, L., Meng, D., Zhao, Q., and Xu, Z., "Integration of 3 dimensional discrete wavelet transform and Markov random field for hyperspectral image classification," *Neurocomputing*, vol. 226, pp. 90-100, 2017.
- [4] Chen, Y., Jiang, H., and P.Ghamisi, "Deep feature extraction and classification of hyperspectral images based on convolutional neural networks," *IEEE Transactions on Geoscience and Remote Sensing.*, vol. 54, no. 10, pp. 6232-6251, 2016.
- [5] Chen, Y., Lin, Z., and Gu, Y., "Deep learning based classification of hyperspectral data," *IEEE Journal of Selected Topics in Applied Earth Observations and Remote Sensing*, vol. 7, no. 6, pp. 2094 – 2107, 2014.
- [6] Chen, Y., Zhao, X., and Jia, X. "Spectral-spatial classification of hyperspectral data based on deep belief network," *IEEE Journal Selected Topics Application Earth Observation Remote Sensing.*, vol. 8, no. 6, pp. 2381–2392, 2015.
- [7] Fahim Irfan Alam, Jun zhou, "Conditional Random Field and Deep Feature learning for hyperspectral image classification," *IEEE Transactions on Geoscience and Remote Sensing.*, vol. 57, no. 3 pp. 1612 - 1628, 2019.
- [8] Fauvel, M., Benediktsson, J., Chanussot, J.,and Sveinsson, J., "Spectral and spatial classification of hyperspectral data using SVMs and morphological profiles," *IEEE Transactions on Geoscience and Remote Sensing.*, vol. 46, no. 11, pp. 3804–3814, 2008.
- [9] Ghamisi, P., Dalla Mura, M., Benediktsson, J.A, "A survey on spectral–spatial classification techniques based on attribute profiles," *IEEE Transactions on Geoscience and Remote Sensing.*, vol. 53, no. 11, pp. 2335–2353, 2015.
- [10] Hughes, F., "On the mean accuracy of statistical pattern recognizers," *IEEE Transaction information Theory*, vol. 14, no. 1, pp. 55-63, 1968.
- [11] Ji, S., Xu, W., Yang, M., and Yu, K., "3D convolutional neural networks for human action recognition," *IEEE Transaction Pattern Analysis Machine Intelligence.*, vol. 35, no. 1, pp. 221–231, 2013.
- [12] Kaiqiang Zhu, Yushi Chen, and Pedram Ghamisi, "Deep Convolutional Capsule Network for Hyperspectral Image Spectral and Spectral-Spatial Classification," *Remote Sens.* 2019.
- [13] Kolmogorov, V., and R. Zabini, R., "What energy functions can be minimized via graph cuts," *IEEE transactions on pattern analysis and machine intelligence*, vol. 26, no. 2, pp. 147–159, 2004.
- [14] Lee, H., and Kwon, H., "Contextual deep CNN based hyperspectral classification," In *Proceedings of the 2014 IEEE Geoscience and Remote Sensing Symposium.*, pp. 3322–3325, 2016.
- [15] Li, J., Bioucas-Dias, J. M., and Plaza, A., "Spectral–spatial hyperspectral image segmentation using subspace multinomiallogistic regression and Markov random fields," *IEEE Transactions on Geoscience and Remote Sensing.*, vol. 50, no. 3, pp. 809–823, 2012.

- [16] Li, J., Bioucas-Dias, J. M., and Plaza, A., "Hyperspectral image segmentation using new Bayesian approach with active learning," IEEE Transactions on Geoscience and Remote Sensing., vol. 49, no. 10, pp. 3947-3960. 2011.
- [17] Li Wang, Jiangtao Peng, and Weiwei Sun, "Spatial-Spectral Squeeze-and-Excitation Residual Network for Hyperspectral Image Classification," Remote Sens. 2019.
- [18] Li, Y., Zhang, H., and Shen, Q., "Spectral-spatial classification of hyperspectral imagery with 3D convolutional neural network," Remote Sensing., vol. 9, no. 1, p. 67, 2017.
- [19] Lin Zhu, Yushi Chen, and Pedram Ghamisi, "Generative Adversarial Networks for hyperspectral image classification", IEEE Transactions on Geoscience and Remote Sensing, vol. 9, no. 1, p. 56, 2018.
- [20] Luo, B., Yang, C., and Zhang, L., "Crop yield estimation based on unsupervised linear unmixing of multirate hyperspectral imagery," IEEE Transactions on Geoscience and Remote Sensing., vol. 51, no. 1, pp. 162-173, 2013.
- [21] Mou, L., Ghamisi, p., and Zhu, X., "Deep recurrent neural networks for hyperspectral image classification," IEEE Transactions on Geoscience and Remote Sensing., vol. 55, no. 7, pp. 3639 - 3655, 2017.
- [22] Melgami, F., and Bruzzone, L., "Classification of hyperspectral remote sensing images with support vector machines," IEEE Transactions on Geoscience and Remote Sensing ., vol. 42, no.8, pp. 1778-1790, 2004.
- [23] Muhammad Ahmada, Sidrah Shabbirb, Diego Olivac , and Manuel Mazzarad , "Spatial-prior generalized fuzziness extreme learning machine autoencoder-based active learning for hyperspectral image classification," International Journal for Light and Electron Optics, vol. 206, Elsevier. 163712, 2020.
- [24] Pedram ghamisi, and Yushi Chen, "A self improving convolutional neural network for the classification of hyperspectral data," IEEE Geoscience and remote sensing letter., vol. 13, no. 10, pp. 1537 - 1541, 2016.
- [25] Qin Xu , Yong Xiao, Dongyue Wang and Bin Luo, "CSA-MSO3DCNN: Multiscale Octave 3D-CNN with Channel and Spatial Attention for Hyperspectral Image Classification," Remote Sens. 2020
- [26] Radhesyam Vaddi, Prabukumar Manoharan, "Hyperspectral image classification using CNN with spectral and spatial features integration," Infrared Physics and Technology, vol. 107, Elsevier, 2020.
- [27] Shaohui Mei, Xin Yuan , Jingyu Ji, " Hyperspectral image spatial Resolution via 3D full convolutional neural network," Remote Sensing., vol.11, no. 9, pp.1139-1152, 2017.
- [28] Shelhamer, E., Long, J and Darrell, T., "Fully convolutional networks for semantic segmentation," Proceedings of the IEEE Conference on Computer Vision and Pattern Recognition (CVPR), pp. 3431- 3440, 2015.
- [29] Tarabalka, Y., Chanussot, J., and Benediktsson, J., "Segmentation and classification of hyperspectral images using watershed transformation," Pattern Recognition., vol. 43, no. 7, pp. 2367-2379, 2010.
- [30] Tarabalka, Y., Rana, A., "A graph cut based model for spectral-spatial classification of hyperspectral images," In Proceedings of the 2014 IEEE Geoscience and Remote Sensing Symposium, Quebec, QC, Canada,13-18, pp. 3418- 3421, 2014.
- [31] Wenchao Qi, Xia Zhang, Nan Wang, Mao Zhang and Yi Cen, "A Spectral-Spatial Cascaded 3D Convolutional Neural Network with a Convolutional Long Short-Term Memory Network for Hyperspectral Image Classification," Remote Sens. 2019.
- [32] Xiangyong Cao, Feng Zhou, lin Xu, " Hyperspectral image segmentation with Markov random Fields and a convolutional neural networks," IEEE Transaction on Image Processing., vol. 27, no. 5, pp. 2354 - 2367, 2018.
- [33] Yang, X., and Yu, Y., "Estimating soil salinity under various moisture conditions: An experimental study," IEEE Transactions on Geoscience and Remote Sensing., vol. 55, no. 5, pp. 2525-2533, 2017.
- [34] Yedidia, J., Freeman, W., and Weiss, Y., "Constructing free-energy approximations and generalized belief propagation algorithms," IEEE Transactions on Information Theory, vol. 51, no. 7, pp. 2282-2312, 2005.
- [35] Yue, J., Zhao, W., Mao, S., and Liu, H., "Spectral- spatial classification of hyperspectral image using deep convolutional neural network," Remote Sensing Letters, vol. 6, no. 6, pp. 468-477, 2015.



**15<sup>th</sup> & 16<sup>th</sup> September 2021**

**Organized by**

**Department of Computer Science, Parvathy's Arts and Science College, Dindigul, Tamilnadu, India**

- [36] Zilong Zhong, Jonathan Li, Zhiming Luo, "Spectral-spatial residual network for hyperspectral image classification: A 3D deep learning framework," IEEE Transactions on Geoscience and Remote Sensing., vol. 56, no. 2, pp. 847 - 858 , 2018.
- [37] Zhao, W., and Du, S., "Spectral-spatial Feature extraction for hyperspectral image classification: A dimension reduction and deep learning approach," IEEE Transactions on Geoscience and Remote Sensing., vol. 54, no. 8, pp. 4544-4554,2016.



**Impact Factor:  
7.569**



# INTERNATIONAL JOURNAL OF INNOVATIVE RESEARCH

IN SCIENCE | ENGINEERING | TECHNOLOGY

 9940 572 462  6381 907 438  [ijirset@gmail.com](mailto:ijirset@gmail.com)



[www.ijirset.com](http://www.ijirset.com)

Scan to save the contact details